PHOTONICS Research

MOVPE-grown AlGaN-based tunnel heterojunctions enabling fully transparent UVC LEDs

Christian Kuhn,[1,*] Luca Sulmoni,[1] Martin Guttmann,[1] Johannes Glaab,[2] Norman Susilo,[1] Tim Wernicke,[1] Markus Weyers,[2] and Michael Kneissl[1,2]

[1]Technische Universität Berlin, Institute of Solid State Physics, Hardenbergstr. 36, EW6-1, 10623 Berlin, Germany
[2]Ferdinand-Braun-Institut, Leibniz-Institut für Höchstfrequenztechnik, Gustav-Kirchhoff-Str. 4, 12489 Berlin, Germany
*Corresponding author: christian.kuhn@physik.tu-berlin.de

Received 7 January 2019; revised 12 February 2019; accepted 25 February 2019; posted 26 February 2019 (Doc. ID 356525); published 29 April 2019

We report on AlGaN-based tunnel heterojunctions grown by metalorganic vapor phase epitaxy enabling fully transparent UVC LEDs by eliminating the absorbing p-AlGaN and p-GaN layers. Furthermore, the electrical characteristics can be improved by exploiting the higher conductivity of n-AlGaN layers as well as a lower resistance of n-contacts. UVC LEDs with AlGaN:Mg/AlGaN:Si tunnel junctions exhibiting single peak emission at 268 nm have been realized, demonstrating effective carrier injection into the AlGaN multiple quantum well active region. The incorporation of a low band gap interlayer enables effective tunneling and strong voltage reduction. Therefore, the interlayer thickness is systematically varied. Tunnel heterojunction LEDs with an 8 nm thick GaN interlayer exhibit continuous-wave emission powers >3 mW near thermal rollover. External quantum efficiencies of 1.4% at a DC current of 5 mA and operating voltages of 20 V are measured on-wafer. Laterally homogeneous emission is demonstrated by UV-sensitive electroluminescence microscopy images. The complete UVC LED heterostructure is grown in a single epitaxy process including *in situ* activation of the magnesium acceptors. ©2019 Chinese Laser Press

https://doi.org/10.1364/PRJ.7.0000B7

1. INTRODUCTION

UVC LEDs with high output power and efficiency are needed for application in water purification, disinfection of surfaces and medical equipment, as well as sensing [1]. One main challenge limiting the performance of UVC LEDs is the strongly absorbing GaN:Mg layer, which is typically employed to achieve decent p-contact resistances [2]. By incorporating UV-transparent AlGaN:Mg and UV-reflective p-contact metals, flip-chip mounted UVC LEDs with external quantum efficiencies (EQEs) exceeding 20% have been demonstrated [3]. However, this typically results in higher operating voltages, since the fabrication of UV-reflective ohmic contacts to AlGaN:Mg layers is very challenging, leading to high contact resistances, accordingly increased Joule heating and device degradation. One interesting approach to overcome these challenges is the implementation of a tunnel junction (TJ), initially discovered by Esaki [4], in reverse bias configuration [5]. In tunnel heterojunction UVC LEDs, the UV-absorbing AlGaN:Mg and GaN:Mg layers are eliminated and replaced by a thin low band gap TJ interlayer and a UV-transparent AlGaN:Si top current spreading layer. For example, by combining a UV-transparent AlGaN:Si layer with a 1 nm to 8 nm thin GaN interlayer, the UV light absorption can be strongly reduced. This configuration can also enable improved light extraction efficiency (LEE) in combination with UV-reflective contacts as well as high wall-plug efficiency, if tunneling with a small voltage drop can be achieved. The higher resistive metal contacts to AlGaN:Mg would then be replaced by low resistive contacts to AlGaN:Si. The efficient current spreading in AlGaN:Si could then be used to incorporate a UV-reflector for enhanced LEE. Further advantages result in a fast and simplified as well as more efficient TJ-LED fabrication process demanding just two lithography masks, one for mesa etching and one for the metal stack, thus enabling simultaneous deposition and annealing of the top and bottom n-contacts. As a future perspective, AlGaN-based TJs could be used to realize UV laser diodes (LDs) with lateral current injection via buried TJs as reported for InGaN-based LDs [6], or cascaded UV LEDs with multiple active regions connected via TJs.

Several groups have reported visible LEDs and LDs with molecular beam epitaxy (MBE)-grown or regrown TJs [7–11]. Metalorganic vapor phase epitaxy (MOVPE)-grown TJ LEDs

have been demonstrated in the GaN/GaN material system (tunnel homojunction) [12–14] as well as in the InGaN/GaN material system (tunnel heterojunction) [11,15–17]. In the AlGaN material system, reduced tunneling probabilities are expected due to the very large band gap of AlGaN with high aluminum mole fraction [5]. Nevertheless, MBE-grown AlGaN-based tunnel heterojunctions combined with UV LEDs have been demonstrated by Zhang *et al.* [18,19]. Furthermore, simulations of AlGaN-based TJ-LEDs indicate that sufficient tunnel current can be obtained if the TJ heterostructure design is carefully optimized, including layer thicknesses, graded AlGaN compositions, and doping profiles [20]. In this paper, we will demonstrate TJ-LEDs with emission in the deep UV spectral region exclusively grown by MOVPE.

2. EXPERIMENT

The TJ-LEDs were grown within a $3 \times 2''$ close-coupled showerhead MOVPE reactor with ammonia (NH_3), trimethylaluminum (TMAl), and trimethylgallium (TMGa) as precursors, silane (SiH_4) and cyclopentadienylmagnesium (Cp2Mg) as dopant sources, as well as hydrogen (H_2) and nitrogen (N_2) as carrier gases. The heterostructures were grown on epitaxially laterally overgrown (ELO) AlN on (0001) sapphire substrates with a threading dislocation density (TDD) of $1–2 \times 10^9$ cm^{-2} and a miscut of 0.1° towards the $[1\bar{1}00]$ sapphire direction [21,22]. The UV LED heterostructure, schematically shown in Fig. 1(a) with simulation of the band profile at 0 V bias voltage in Fig. 1(b), consists of an AlGaN:Si bottom current spreading layer with interface grading followed by a threefold quantum well (TQW) active region using 5 nm thick $Al_{0.63}Ga_{0.37}N$ barriers and 2.2 nm thick $Al_{0.48}Ga_{0.52}N$ QWs, designed for emission near 270 nm. The AlGaN TQW active region is followed by a 5 nm thick $Al_{0.85}Ga_{0.15}N$ electron blocking layer and a 100 nm thick AlGaN:Mg-based short-period superlattice (SPSL) with average aluminum mole fraction of 75%. The subsequently grown TJ is composed of 20 nm $Al_{0.75}Ga_{0.25}N:Mg^{2+}$ SPSL ($[Mg] = 9 \times 10^{19}$ cm^{-3}) and 15 nm $Al_{0.65}Ga_{0.35}N:Si^{2+}$ ($[Si] = 5 \times 10^{19}$ cm^{-3}) followed by a 300 nm thick $Al_{0.65}Ga_{0.35}N$:Si top current spreading layer. After AlGaN:Mg^{2+} SPSL growth, the structures were *in situ* thermally annealed under nitrogen to activate the Mg acceptors. In the case of the tunnel heterojunction experiment, we incorporated a GaN:Si interlayer with varying nominal thicknesses $d = 1$ nm, 4 nm, and 8 nm between the AlGaN:Mg^{2+}/AlGaN:Si^{2+}-layers. The growth rate of 130 nm/h was calibrated on a thick GaN layer using *in situ* reflectometry. However, due to the large lattice mismatch of such GaN layer to the underlying AlGaN layers strained to AlN, the GaN layer is expected to perform a transition from two-dimensional to three-dimensional growth accompanied by relaxation at a certain critical thickness within the nanometer range [23,24]. Following the MOVPE growth, TJ-LEDs were fabricated with standard processing techniques. First, mesa structures with square and finger geometries were formed by dry-etching down to the bottom n-AlGaN current spreading layer, followed by the simultaneous deposition of a V/Al/Ni/Au n-contact metal stack with frame and stripe geometry on top and bottom AlGaN:Si layers. The n-contacts were subsequentially annealed at 800°C in nitrogen atmosphere. The electroluminescence (EL) characterization was performed on-wafer at room temperature without active cooling by measuring voltage versus current and light output power versus current for bottom emission using a calibrated UV-enhanced Si photodiode. Top and bottom spectral properties were measured using a calibrated compact spectrometer. Furthermore, the EL distribution in the QW plane of the TJ-LED, measured through the top side, was characterized with a UV-sensitive microscopic camera system.

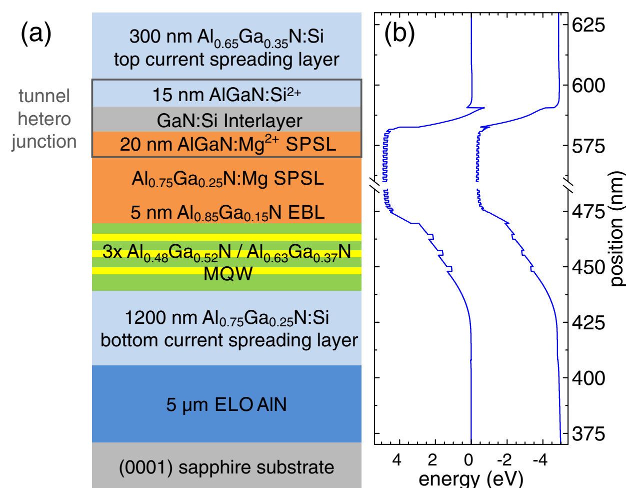

Fig. 1. (a) Schematic of a UVC LED with a tunnel heterojunction in reverse bias configuration for hole injection. (b) Equilibrium band structure diagram (0 V bias voltage) of a TJ-LED with 8 nm GaN:Si interlayer.

3. RESULTS AND DISCUSSION

In Fig. 2(a), emission spectra measured through the substrate of UVC LEDs with TJs are shown, exhibiting a clear QW peak at 268 nm. Emission spectra measured from the top are basically identical, although the top emission power is lower due to higher internal reflection at the interface between AlGaN:Si and air. All TJ-LEDs that included an interlayer proved to be functional. Even for the tunnel homojunction LEDs (without interlayer), carrier injection was possible and UVC light emission was observed. The inset in Fig. 2 shows microscope images of a TJ-LED before operation [Fig. 2(b)] and during operation [Fig. 2(c)]. Due to the UV-transparent top AlGaN:Si current spreading layer, the QW luminescence can be measured from the top and appears in "blue" color in this microscope image.

In order to investigate the homogeneity of current spreading and current injection, the top emission from the TJ-LED was imaged by a UV-sensitive camera at a continuous-wave (cw) current of 5 mA (Fig. 3). In Fig. 3(a), square mesa geometry with frame top n-contact and in Fig. 3(b) finger-shaped mesa geometry with a central stripe top n-contact are shown, both with a total emitting area of 0.1 mm^2. The electric top contact is provided by the small metal electrodes (frame or stripe) only. The LEDs exhibit a homogeneous lateral distribution of the 268 nm emission from the square mesa [Fig. 3(a)]

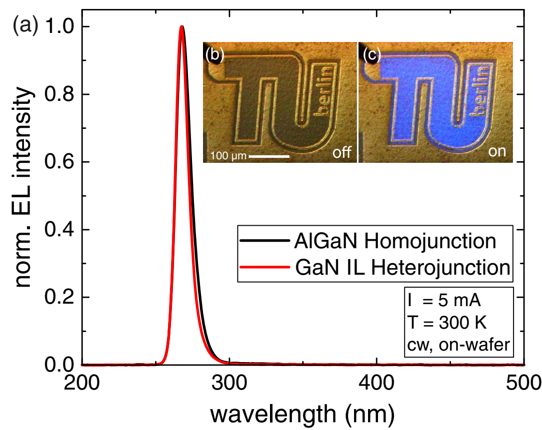

Fig. 2. (a) Normalized emission spectra of fully transparent MOVPE-grown TJ-LEDs with GaN interlayer (heterojunction) and without interlayer (homojunction) emitting at 268 nm. The inset shows microscope images of the heterojunction TJ-LED in (b) the "off" state and (c) the "on" state of the device.

indicating a homogeneous current injection via the tunnel heterojunction combined with uniform Mg acceptor activation of the buried AlGaN:Mg. Secondary ion mass spectrometry profiles of comparable TJ-LED samples exhibit hydrogen concentrations in the range of 10%-15% of the Mg concentration in the AlGaN:Mg and AlGaN:Mg^{2+} layers, indicating only a partial passivation of Mg acceptors during growth or AlGaN:Si overgrowth using ammonia. However, this partial passivation might affect the operation voltage of the devices. A slight intensity enhancement near the central stripe contact of the mesa with finger geometry [Fig. 3(b)] indicates insufficient current spreading of the top AlGaN:Si layer. Similar $Al_xGa_{1-x}N$:Si layers with $0.6 \leq x \leq 0.8$ exhibit resistivities of $\rho_s = 0.025\ \Omega \cdot \mathrm{cm}$ [25], whereas the resistivity of the top $Al_{0.65}Ga_{0.35}N$:Si layer of the TJ-LED has been estimated by transfer length method (TLM) measurements to be $\rho_s = 0.03\ \Omega \cdot \mathrm{cm}$. The slight increase in resistivity indicates a partial Si donor compensation, caused by magnesium incorporation during the growth of AlGaN:Si subsequent to AlGaN:Mg growth.

In Fig. 4, current-voltage and current-emission power (LIV) measurements of TJ-LEDs with homojunction as well as with GaN:Si interlayer thicknesses of 1 nm, 4 nm, and 8 nm are shown for a finger-shaped geometry with 0.15 mm^2 mesa size and central stripe top n-contact. All TJ-LEDs exhibit similar levels of bottom emission power in the range of 1.4 mW to 1.7 mW at a cw current of 20 mA. Peak output powers of more than 3 mW near thermal rollover have been obtained for the sample with 8 nm interlayer thickness. For low currents, the emission power increases linearly without any indication of non-radiative current paths or carrier leakage. However, the operation voltage of the TJ-LEDs is strongly affected by the interlayer. With increasing interlayer thickness, the TJ-LED operation voltage is strongly reduced, shown in Fig. 5 for a current of 5 mA ($j = 3\ \mathrm{A/cm^2}$). TJ-LEDs without an interlayer or with very thin interlayers exhibit very high voltages (almost 40 V), which is due to very inefficient tunneling, causing device breakthrough already below 60 mA. The voltage decreases to 20 V at 5 mA for the sample with 8 nm thick interlayer. For such thick interlayers, the reduced operating voltages enable higher emission powers in the high current range due to less thermal heating. These structures then benefit from lower internal resistance, which leads to higher wall-plug efficiency (WPE). This demonstrates that the thickness of the interlayer is one of the most crucial parameters for efficient tunneling injection in TJ-LED heterostructures and needs to be accurately adjusted, as it influences polarization fields, relaxation mechanisms, and decisively the tunneling probabilities. For this first demonstration, the AlGaN composition profile and the doping profile of the TJ have not been fully optimized. Nevertheless, these operation voltages are similar to or even lower than UVC LEDs with wide band gap AlGaN:Mg SPSL p-layers with aluminum mole fraction higher than 70% [26]. The resistance of a TJ can be estimated by evaluating the differential device resistance (dV/dj) of a TJ-LED at elevated current density [20].

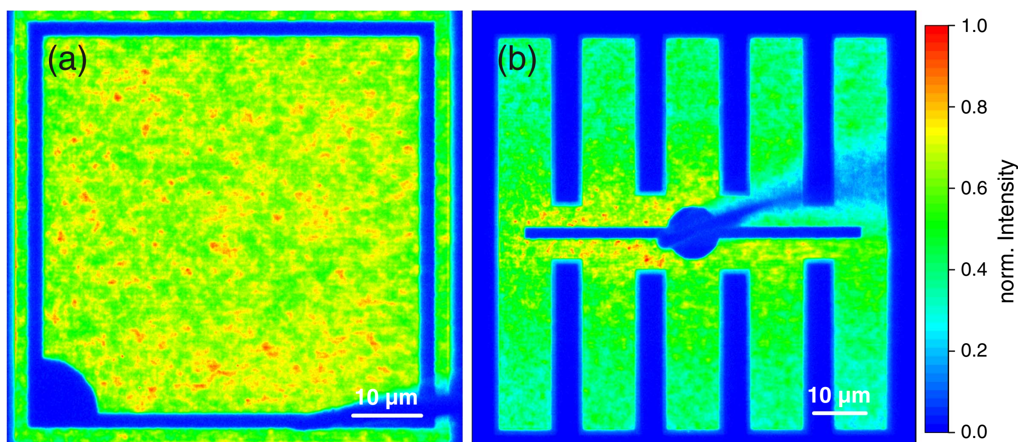

Fig. 3. Microscope images taken by a UV-sensitive camera for TJ-LEDs at a DC current of 5 mA. (a) A square mesa geometry with a top n-contact at the perimeter and (b) a finger-shaped mesa geometry with central stripe top n-contact are measured from the top. The electric contact is provided by the small metal electrodes only. The entire mesa area of the top AlGaN:Si semiconductor is homogeneously emitting with a slight enhancement under the stripe contact.

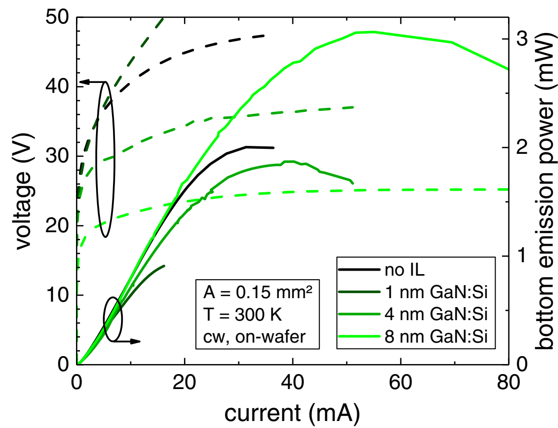

Fig. 4. Experimental LIV curves for tunnel heterojunction LEDs with emitting area of 0.15 mm^2 featuring 1, 4, and 8 nm thick interlayers as a function of the injected current under cw operation. The black curves represent the tunnel homojunction LED.

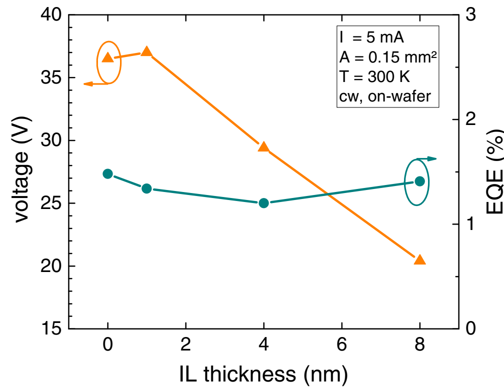

Fig. 5. Operation voltage and external quantum efficiency in bottom emission configuration of UVC LEDs with tunnel junction measured at a cw current of 5 mA as a function of the interlayer thickness.

This device resistance is an upper estimate for TJ resistance, as other layers can significantly contribute to the device resistance, such as n-contacts or the p-layers. The contact resistivity ρ_c of ohmic top n-contacts of the TJ-LEDs has been estimated by TLM measurements to be $\rho_c = 0.001\ \Omega \cdot \mathrm{cm}^2$. 50 μm × 50 μm-sized TJ-LEDs with an 8 nm GaN:Si interlayer exhibit a device resistance of $4\text{–}6 \times 10^{-3}\ \Omega \cdot \mathrm{cm}^2$ at 350 $\mathrm{A/cm}^2$, which is in the same order of magnitude as reported TJs for hole injection into wide band gap AlGaN:Mg layers with aluminum content above 70% [19]. The EQE, however, is nearly constant within this variation of interlayer thickness (Fig. 5): EQE = 1.2% to 1.4% at 5 mA in bottom emission configuration. The current experiment does not show a reduction in EQE with increasing GaN layer thickness, even though absorption in the low band gap interlayer could reduce the emitted light intensity. However, variation of the measured EQE is as large as the reduction in LEE by 16% expected for an 8 nm GaN layer. Furthermore, confinement and electric fields might additionally influence the absorption properties of the interlayer. In cw operation, the maximum EQE of 1.9% was achieved before thermal rollover at 20 mA. On the other hand, in pulsed operation, EQE values exceeding 2.3% and emission power of more than 6 mW at 60 mA were achieved on-wafer. Maximum WPEs of WPE = 0.41% in cw operation as well as WPE = 0.45% in pulsed operation have been obtained at 8 mA, all measured by a large-area Si-photodiode below the substrate. In order to determine the total emission power including light emitted through the top side, TJ-LEDs were measured in a calibrated integrating sphere (Ulbricht sphere) at a fixed cw current. In this measurement, a total emission power of 0.53 mW, EQE of 2.3%, as well as WPE of 0.54% have been obtained at 5 mA. Compared to measurements in bottom emission configuration, the total EQE is enhanced by a factor of 1.8 due to light emitted through the transparent top side of the TJ-LEDs.

4. CONCLUSION

In summary, we demonstrated MOVPE-grown AlGaN-based TJs enabling fully transparent UVC LEDs. Even for TJ-LEDs without interlayers, carrier injection and UVC light emission were possible, at the cost of very high voltages. This is the first demonstration of an AlGaN/AlGaN homojunction in literature. We also confirmed the reduction in operation voltages when implementing a GaN interlayer with smaller band gap. The lowest voltage of 20 V at 5 mA was achieved for 8 nm thick interlayers. These TJ-LEDs exhibit single peak emission at 268 nm without parasitic emission. Emission power of 1.7 mW and EQE of 1.9% were achieved at 20 mA in cw operation as well as EQE values of 2.3% and emission power of more than 6 mW at 60 mA in pulsed operation, all measured on-wafer. The complete UVC LED with tunnel heterojunction was grown in a single MOVPE step, which would be the method of choice for industrial LED fabrication.

Funding. Bundesministerium für Bildung und Forschung (BMBF) "Advanced UV for Life" Project (03ZZ0134C); Deutsche Forschungsgemeinschaft (DFG) Collaborative Research Centre "Semiconductor Nanophotonics" (CRC787 9315).

Acknowledgment. The authors would like to thank Tetsuya Takeuchi for detailed discussion, Sylvia Hagedorn for ELO template supply, Verena Montag for device characterization, as well as Praphat Sonka for technical assistance. The authors declare that there are no conflicts of interest related to this article.

REFERENCES

1. M. Kneissl and J. Rass, eds., *III-Nitride Ultraviolet Emitters: Technology and Applications* (Springer, 2016).
2. N. Susilo, J. Enslin, L. Sulmoni, M. Guttmann, U. Zeimer, T. Wernicke, M. Weyers, and M. Kneissl, "Effect of the GaN:Mg contact layer on the light-output and current-voltage characteristic of UVB LEDs," Phys. Status Solidi A **215**, 1700643 (2017).
3. T. Takano, T. Mino, J. Sakai, N. Noguchi, K. Tsubaki, and H. Hirayama, "Deep-ultraviolet light-emitting diodes with external quantum efficiency higher than 20% at 275 nm achieved by improving light-extraction efficiency," Appl. Phys. Express **10**, 031002 (2017).
4. L. Esaki, "New phenomenon in narrow germanium p-n junctions," Phys. Rev. **109**, 603–604 (1958).

5. S. Rajan and T. Takeuchi, "III-nitride tunnel junctions and their applications," in *III-Nitride Based Light Emitting Diodes and Applications* (Springer, 2017), pp. 209–238.
6. M. Malinverni, C. Tardy, M. Rossetti, A. Castiglia, M. Duelk, C. Velez, D. Martin, and N. Grandjean, "InGaN laser diode with metal-free laser ridge using n^+-GaN contact layers," Appl. Phys. Express **9**, 061004 (2016).
7. M. Malinverni, D. Martin, and N. Grandjean, "InGaN based micro light emitting diodes featuring a buried GaN tunnel junction," Appl. Phys. Lett. **107**, 051107 (2015).
8. S. M. Sadaf, Y.-H. Ra, H. P. T. Nguyen, M. Djavid, and Z. Mi, "Alternating-current InGaN/GaN tunnel junction nanowire white light emitting diodes," Nano Lett. **15**, 6696–6701 (2015).
9. E. C. Young, B. P. Yonkee, F. Wu, S. H. Oh, S. P. DenBaars, S. Nakamura, and J. S. Speck, "Hybrid tunnel junction contacts to III-nitride light emitting diodes," Appl. Phys. Express **9**, 022102 (2016).
10. C. Skierbiszewski, G. Muziol, K. Nowakowski-Szkudlarek, H. Turski, M. Siekacz, A. Feduniewicz-Zmuda, A. Nowakowska-Szkudlarek, M. Sawicka, and P. Perlin, "True-blue laser diodes with tunnel junctions grown monolithically by plasma-assisted molecular beam epitaxy," Appl. Phys. Express **11**, 034103 (2018).
11. M. J. Grundmann and U. K. Mishra, "Multi-color light emitting diode using polarization-induced tunnel junctions," Phys. Status Solidi C **4**, 2830–2833 (2007).
12. S.-R. Jeon, Y.-H. Song, H.-J. Jang, and G. M. Yang, "Lateral current spreading in GaN-based light-emitting diodes utilizing tunnel contact junctions," Appl. Phys. Lett. **78**, 3265–3267 (2001).
13. S. Neugebauer, M. P. Hoffmann, H. Witte, J. Bläsing, A. Dadgar, A. Strittmatter, T. Niermann, M. Narodovitch, and M. Lehmann, "All metalorganic chemical vapor phase epitaxy of p/n-GaN tunnel junction for blue light emitting diode applications," Appl. Phys. Lett. **110**, 102104 (2017).
14. D. Hwang, A. J. Mughal, M. S. Wong, A. I. Alhassan, S. Nakamura, and S. P. DenBaars, "Micro-light-emitting diodes with III-nitride tunnel junction contacts grown by metalorganic chemical vapor deposition," Appl. Phys. Express **11**, 012102 (2018).
15. T. Takeuchi, G. Hasnain, S. Corzine, M. Hueschen, J. R. P. Schneider, C. Kocot, M. Blomqvist, Y. I. Chang, D. Lefforge, M. R. Krames, L. W. Cook, and S. A. Stockman, "GaN-based light emitting diodes with tunnel junctions," Jpn. J. Appl. Phys. **40**, L861 (2001).
16. M. Diagne, Y. He, H. Zhou, E. Makarona, A. V. Nurmikko, J. Han, K. E. Waldrip, J. J. Figiel, T. Takeuchi, and M. Krames, "Vertical cavity violet light emitting diode incorporating an aluminum gallium nitride distributed Bragg mirror and a tunnel junction," Appl. Phys. Lett. **79**, 3720–3722 (2001).
17. Y. Kuwano, M. Kaga, T. Morita, K. Yamashita, K. Yagi, M. Iwaya, T. Takeuchi, S. Kamiyama, and I. Akasaki, "Lateral hydrogen diffusion at p-GaN layers in nitride-based light emitting diodes with tunnel junctions," Jpn. J. Appl. Phys. **52**, 08JK12 (2013).
18. Y. Zhang, S. Krishnamoorthy, J. M. Johnson, F. Akyol, A. Allerman, M. W. Moseley, A. Armstrong, J. Hwang, and S. Rajan, "Interband tunneling for hole injection in III-nitride ultraviolet emitters," Appl. Phys. Lett. **106**, 141103 (2015).
19. Y. Zhang, Z. Jamal-Eddine, F. Akyol, S. Bajaj, J. M. Johnson, G. Calderon, A. A. Allerman, M. W. Moseley, A. M. Armstrong, J. Hwang, and S. Rajan, "Tunnel-injected sub 290 nm ultra-violet light emitting diodes with 2.8% external quantum efficiency," Appl. Phys. Lett. **112**, 071107 (2018).
20. Y. Zhang, S. Krishnamoorthy, F. Akyol, A. A. Allerman, M. W. Moseley, A. M. Armstrong, and S. Rajan, "Design and demonstration of ultra-wide bandgap AlGaN tunnel junctions," Appl. Phys. Lett. **109**, 121102 (2016).
21. A. Knauer, A. Mogilatenko, S. Hagedorn, J. Enslin, T. Wernicke, M. Kneissl, and M. Weyers, "Correlation of sapphire off-cut and reduction of defect density in MOVPE grown AlN," Phys. Status Solidi B **253**, 809–813 (2016).
22. A. Knauer, A. Mogilatenko, S. Hagedorn, J. Enslin, T. Wernicke, M. Kneissl, and M. Weyers, "Correlation of sapphire off-cut and reduction of defect density in MOVPE grown AlN," Phys. Status Solidi B **253**, 1228 (2016).
23. K. Bellmann, F. Tabataba-Vakili, T. Wernicke, A. Strittmatter, G. Callsen, A. Hoffmann, and M. Kneissl, "Desorption induced GaN quantum dots on (0001) AlN by MOVPE," Phys. Status Solidi RRL **9**, 526–529 (2015).
24. J. Enslin, F. Mehnke, A. Mogilatenko, K. Bellmann, M. Guttmann, C. Kuhn, J. Rass, N. Lobo-Ploch, T. Wernicke, M. Weyers, and M. Kneissl, "Metamorphic $Al_{0.5}Ga_{0.5}N$:Si on AlN/sapphire for the growth of UVB LEDs," J. Cryst. Growth **464**, 185–189 (2017).
25. C. Kuhn, T. Simoneit, M. Martens, T. Markurt, J. Enslin, F. Mehnke, K. Bellmann, T. Schulz, M. Albrecht, T. Wernicke, and M. Kneissl, "MOVPE growth of smooth and homogeneous $Al_{0.8}Ga_{0.2}N$:Si superlattices as UVC laser cladding layers," Phys. Status Solidi A **215**, 1800005 (2018).
26. M. Martens, C. Kuhn, E. Ziffer, T. Simoneit, V. Kueller, A. Knauer, J. Rass, T. Wernicke, S. Einfeldt, M. Weyers, and M. Kneissl, "Low absorption loss p-AlGaN superlattice cladding layer for current-injection deep ultraviolet laser diodes," Appl. Phys. Lett. **108**, 151108 (2016).